

## **ENERGY STUDY OF A SOLAR ASSISTED HEAT PUMP (SAHP)**

**Author(s):**

L. Herzallah<sup>1</sup>, P. Hermanucz<sup>1</sup>

**Affiliation:**

<sup>1</sup> Institute of Technology, Hungarian University of Agriculture and Life Sciences, 2100 Gödöllő, Páter Károly u. 1., Hungary;

**Email address:**

herzallah.lazhari@stud.uni-mate.hu; hermanucz.peter@uni-mate.hu

**Abstract:** By synergizing solar energy with heat pump technology, this solution represents a stride toward a greener and more sustainable future, reducing reliance on non-renewable energies and promoting cleaner air and a less carbon footprint, simply by using the Solar Assisted Heat Pump (SAHP). In this article, we'll investigate an energy study of a SAHP aiming for further sustainable heating applications, our investigation centres on the system's efficiency and potential energy losses under various conditions: when operating with a single compressor versus two, and comparing the impact of insulation versus its absence, to pinpoint areas for potential system enhancements. Utilizing CoolPack software, we conduct theoretical calculations of the Coefficient Of Performance (COP), aligning our findings with experimental measurements. The results show the importance of the insulation in reducing the losses within the system, we were able to conserve 90 W of heat power when the system was running with one compressor, and about 429 W when both compressors were in operation.

**Keywords:** SAHP, heat pump, system efficiency, insulation, compressor(s), energy loss, CoolPack software

### **1. Introduction**

Climate change poses a significant threat to the future of our planet, mostly caused by the continuous consumption of fossil fuels to meet the energy demands of residential and commercial sectors. The adoption of renewable energy not only serves as a strong response to the effects of global warming but also facilitates the advancement of energy optimization. Embracing renewable energy solutions, humanity showcases a profound commitment to preserving the environment for upcoming generations while positioning ourselves to potentially reap the advantages of reduced energy costs [1]. The European Union (EU) has emphasized the importance of energy efficiency and renewable energy in its strategic plan for sustainable development, recognizing the various challenges associated with this goal. The EU Emission Trading Scheme (ETS) serves as evidence of the EU's commitment to reducing emissions, particularly in the domains of electricity generation and large-scale industrial activities [2]. Within this context, the International Energy Agency's 2012 report highlighted the diverse heating and cooling demands across the EU's 27 nations, pinpointing a significant demand for low exergy heat, particularly between 60 °C and 100 °C. Notably, these requirements are common in diverse sectors, covering industries and individuals, for instance, in cold regions (like Budapest), water heating alone contributes to around 15% of the overall energy consumption [3] [4]. Instead of resorting to fossil fuel combustion, a more sustainable and efficient alternative lies in the adoption of heat pump technology.

Heat pumps, already recognized for their pivotal role in heating and cooling homes and various other industrial applications, have seen an impressive uptake but are also very important in swimming pool technology [5], [6]. Between 2010 and 2015, sales figures for electrically driven heat pump units in the EU touched approximately 800,000 units annually [7]. This trend underscores the potential of heat pumps in electrifying heat, presenting a viable alternative to traditional electrical heating. Their inherent efficiency and reduced carbon footprint lend heat pumps a competitive edge [8]. Furthermore, refrigeration emerges as a

dominant player in the broader landscape of energy consumption. Serving a plethora of industries, from food and beverages to chemicals, refrigeration’s utility in processes ranging from cooling to environmental conditioning is undeniable [9]. Combining the power of solar energy with heat pump technology, the SAHP stands out as an innovative alternative. This system excels at cooling and heating by harnessing the sun’s energy to facilitate enhanced heat exchange, boosting overall efficiency. Integrating solar panels, typically solar thermal panels, the SAHP captures solar energy to assist in the heating or pre-heating process. This captured energy can pre-heat the refrigerant, reducing the energy required by the heat pump’s compressor and other components. In a study conducted by [10], a comparative assessment of Flat-Plate Collector (FPC) data was undertaken with a focus on its applications for domestic hot water (DHW). Serving as a real-world example for this investigation was a laboratory at Szent Istvan Campus, located in Gödöllő, Hungary; practical findings from this case study highlighted that the model utilized achieved a commendable 69% solar fraction, corresponding to an annual solar yield of 510 kWh [11]. It’s noteworthy to mention that such technologies hold potential for integration with heat pumps, a domain that has seen significant advancements over the past two decades.

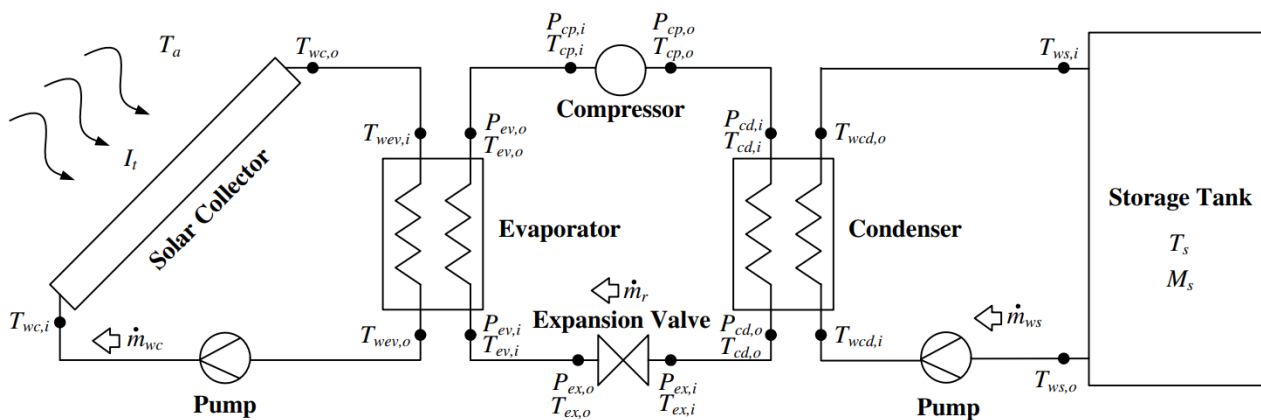


Figure 1. Experimental layout of a SAHP [12]

Figure 1 shows a detailed experimental layout of a SAHP. Water is the liquid used for heat transfer in this setup as referenced in [12]. This medium circulates through the solar panel, facilitating heat transfer from the solar collector to the evaporator and subsequently from the condenser to a storage tank. In certain conditions, it may be necessary to mix water with glycol to prevent freezing when the ambient temperature falls below 0°C [13] [14].

Properly integrating solar thermal collectors with heat pump systems presents a challenge due to the inherent complexities of integration. The inconsistency of solar radiation, influenced by climatic shifts and diurnal cycles, adds another layer of difficulty, prompting researchers to explore advanced control strategies for optimal operation under fluctuating solar conditions. Further, the goal is not only to harness the sun’s energy but to do so efficiently, demanding precise calibration for system optimization in real-time [15]. Simulation tools offer the means to enhance the effectiveness, operation, and configuration of refrigeration cycles. Prior studies have explored the modelling capabilities of heat pumps, as exemplified by [16], who demonstrated the efficient modelling of energy characteristics in cooling circuits using straightforward software like Solkane 7.0. Additionally, alongside Solkane, CoolPack can be used as a simulation tool for the operation of the heat pump and then the SAHP.

## 2. Materials and Methods

### 2.1. Materials and equipment

The experiment took place at the energetic building’s laboratory of the Hungarian University of Agriculture and Life Sciences, spanning four distinct days in July. The experimental setup consists of two primary components: an external flat plate solar collector positioned on the rooftop of the aforementioned building and an internal heat pump situated within the laboratory itself. The integration of these components occurs

at the evaporator level, facilitating the exchange of heat between the antifreeze flowing through the flat plate solar collector and the refrigerant circulating in the heat pump. This interaction enables the efficient transfer of thermal energy between the two blocks. For a visual representation, refer to Figure 2, outlining the experimental configuration.

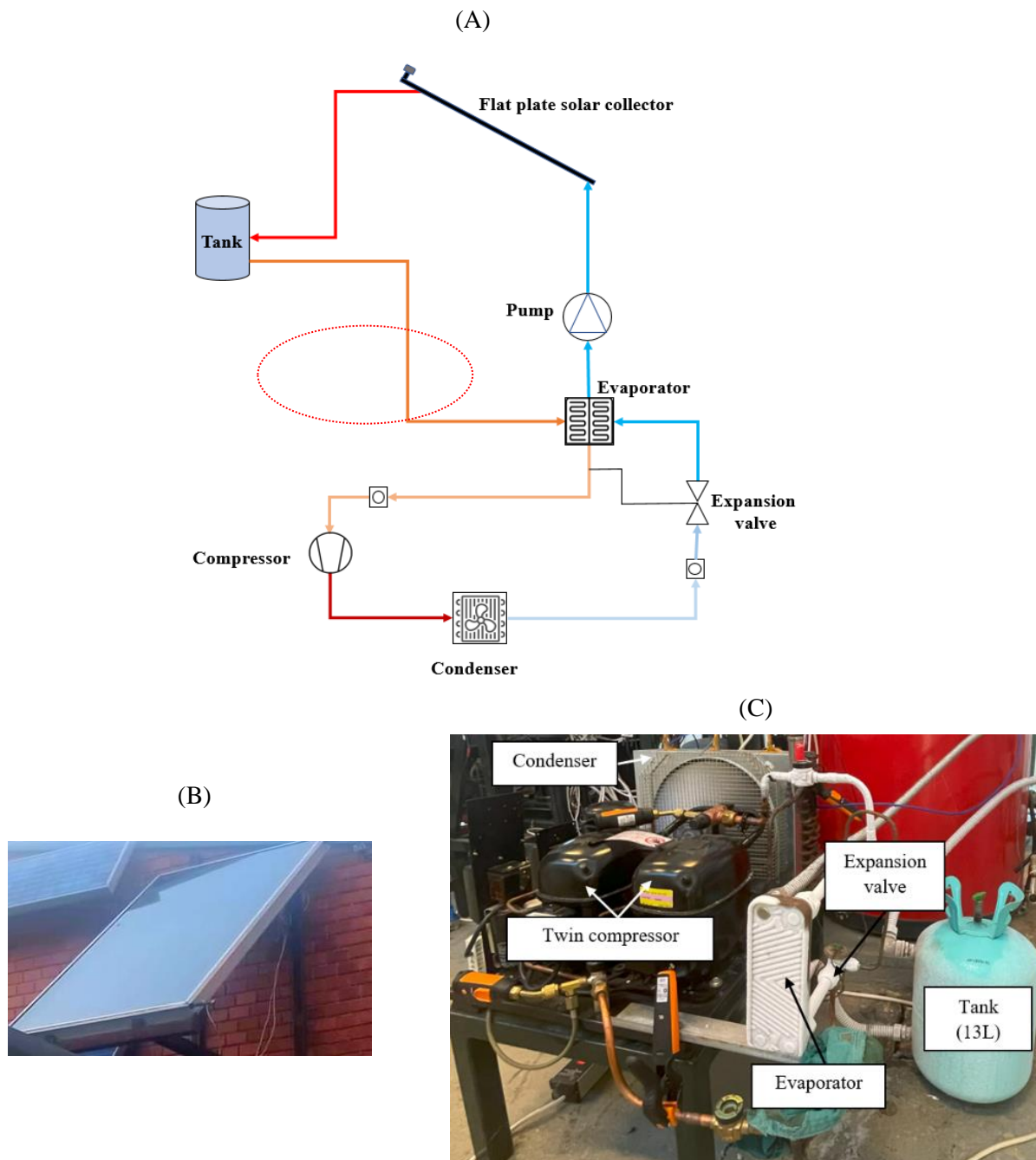


Figure 2. Experimental setup, (A): Schematic diagram, (B): Flat plate solar collector, (C): Heat pump

A flat plate solar collector with a surface area of 1.92 m<sup>2</sup> was used. The collector was thoughtfully positioned facing southwards at a precise angle of 33 degrees concerning the horizontal plane. The primary function of the solar collector was to harness solar energy effectively. A mixture of 70% water and 30% glycol was circulated through a network of tubes positioned within the collector to achieve this. We used a storage tank of 13 liters to serve as a reservoir for storing the heated antifreeze. In the depicted second component, as shown in Figure 2C, which corresponds to the heat pump, a condensing unit equipped with a twin compressor manufactured by the renowned company Danfoss was employed.

## 2.2. Measuring instruments

We strategically positioned multiple sensors and devices in our experimental arrangement to gather essential data and monitor the system's performance. These instruments are presented in Figure 3.

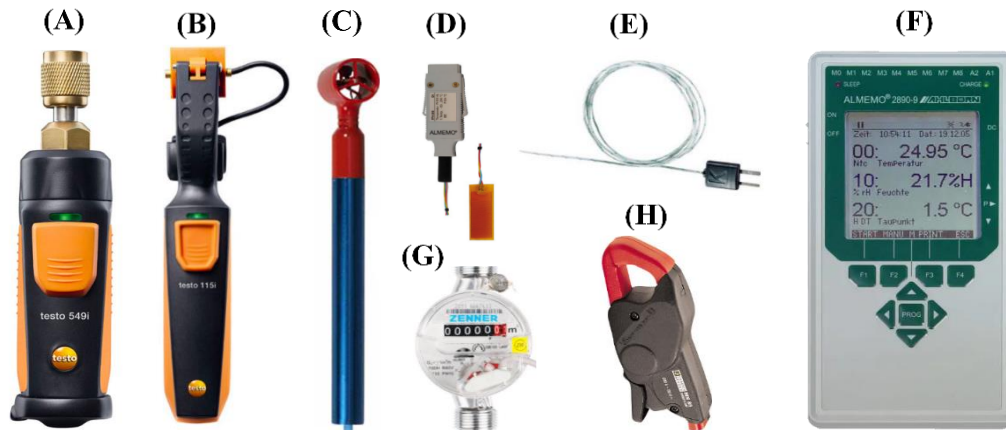


Figure 3. Measuring instruments and sensors, (A): Testo 549i Bluetooth high-pressure gauge, (B): Testo 115i Bluetooth clamp thermometer, (C): Micro rotating vane anemometer, (D): Temperature sensor “Pt 100” type, (E): Temperature sensor “K” type, (F): Data logger, (G): Water meter gauge, (H): Ampere clamp meter

To assess pressure and temperature levels at the compressor(s), we employed two sets of Testo smart probes and clamp thermometers (refer to Figures 3A and 3B). Utilizing Bluetooth technology, we seamlessly transmitted the data on a smartphone. Temperature readings at various system points (outlet and inlet temperature of the solar collector, refrigerant's temperature after passing the condenser, and the airflow temperature at the level of the condenser) were captured through “Pt 100” and “K” type sensors (Figures 3D and 3E). These readings were then integrated into the ALMEMO device (Figure 3F), conveniently displaying results on a connected laptop. For airflow measurement at the condenser back surface (heat outlet), a micro-rotating vane anemometer (Figure 3C) was employed, and the recorded data were stored on a separate data logger. The flow meter (Figure 3G) was strategically positioned vertically on the tubes to measure the flow rate of the antifreeze circulating to the solar collector precisely. To determine the compressor's power consumption, an ampere clamp meter was connected to its power supply (Figure 3H). The ALMEMO system efficiently stored the amperage clamp meter readings obtained during the experiment.

## 2.3. Description of the experiment

In this experiment, we employed an inorganic fibrous material as insulation for the compressor(s), capitalizing on its exceptional thermal properties and non-combustible nature. One of the compressors was covered with this insulation material (Figure 4A), while in another case; we insulated both compressors (Figure 4B) to thoroughly evaluate losses compared with the non-insulated scenario. Besides the compressor(s) insulations, we extended the application to cover the tubes of the heat pump and those connected to the solar collector (inlet and outlet tubes) with rubber insulation pipes, making it an ideal option for ensuring optimal heat transfer and retention within the entire system.

To measure the system's released heat accurately, we arranged nine sensors symmetrically at the condenser's output and added two sensors at its inlet (K-type). Data from these sensors was collected using two ALMEMO devices (Figure 3F). The drawing in Figure 4C demonstrates the division of the condenser's back surface, with each sensor centrally positioned within its section. This strategy enabled us to measure the difference of the air temperature flowing at the level of the condenser, and subsequently, the heat emitted per section. We then summed the heat from each section and applied Equation (2), detailed below, to determine the condenser's total heat discharge.



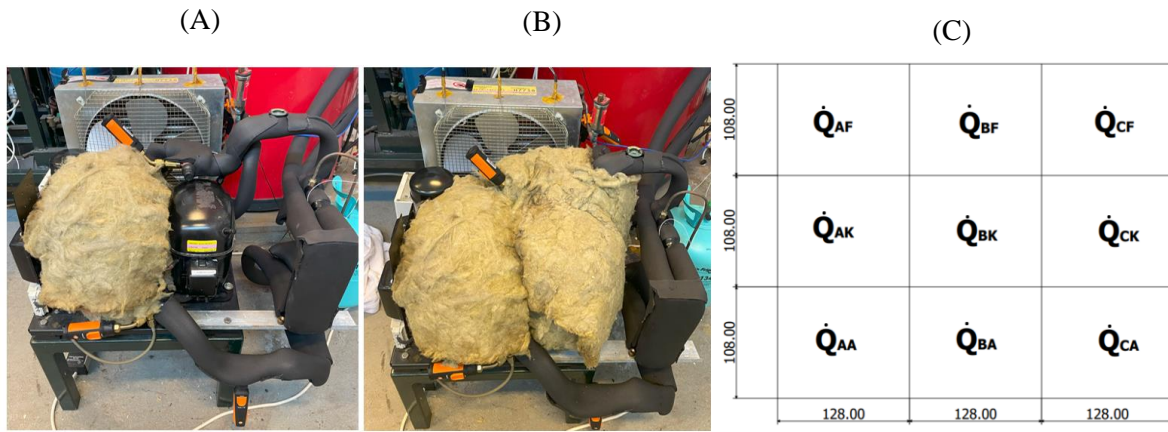


Figure 4. Insulation strategy, (A): Partially insulated system, (B): Totally insulated system. (C): Condenser back surface partitioning in [mm].

The primary objective of insulating the setup was to minimize heat losses during the operation, thereby significantly enhancing the system's overall efficiency. The trials were conducted across a span of four days, for each day different setup was tabulated as follows:

Table 1. Experiments schedule and explanation

Day	Date	Description
1 <sup>st</sup> day	July 14, 2023	One compressor is running without insulation.
2 <sup>nd</sup> day	July 17, 2023	Two compressors are running without insulation.
3 <sup>rd</sup> day	July 24, 2023	One compressor is running with partial insulation (Insulation at the level of one compressor and the tubes).
4 <sup>th</sup> day	July 28, 2023	Two compressors are running with total insulation (Insulation at the level of two compressors and the tubes).

#### 2.4. Adopted calculations

Energy balance equation for the system:

$$\dot{Q}_H = \dot{Q}_S + P_{eff} + E_{loss} \quad (1)$$

Where:

$\dot{Q}_H$ : The total heat flow of the condenser [W], can be calculated as:

$$\dot{Q}_H = \sum_{i=AF}^{CA} \dot{Q}_i = \dot{Q}_{AF} + \dot{Q}_{BF} + \dot{Q}_{CF} + \dot{Q}_{AK} + \dot{Q}_{BK} + \dot{Q}_{CK} + \dot{Q}_{AA} + \dot{Q}_{BA} + \dot{Q}_{CA} \quad (2)$$

The energy released by the condenser per section ( $\dot{Q}_i$ ) could be determined as follows:

$$\dot{Q}_i = \dot{m}_{air} \cdot c_{air} \cdot (T_i - T_{Inlet}) \quad (3)$$

Where:

$\dot{m}_{air}$ : The air's mass flow at the condenser's level [kg/s].

$c_{air}$ : The specific heat capacity of the air [J/kg·°C].

$T_i$ : The outlet air temperature of the specific section of the condenser [°C].

$T_{Inlet}$ : The average inlet air temperature of the condenser [°C].

$\dot{Q}_S$ : The obtained heat from the solar collector [W] can be calculated as follows:

$$\dot{Q}_S = \dot{m}_{Antifreeze} \cdot c_{Antifreeze} \cdot (T_{Outlet} - T_{Inlet}) \quad (4)$$

Where:

$\dot{m}_{Antifreeze}$ : The mass flow of the Antifreeze at the condenser level [kg/s].

$c_{Antifreeze}$ : The specific heat capacity of the antifreeze [J/kg·°C].

$T_i$ : The outlet temperature of the solar collector [°C].

$T_{Inlet}$ : The inlet of the solar collector [°C].

$\dot{Q}_S$ : The obtained heat from the solar collector [W] can be calculated as follows:

$P_{eff}$ : The power consumed by the compressor [W], can be calculated using the following formula:

$$P_{eff} = U_{eff} \cdot I_{eff} \quad (5)$$

Where:

$U_{eff}$ : The voltage from the grid, is equal to 230 [V].

$I_{eff}$ : The consumed current by the compressor(s) [A].

$E_{loss}$ : Energy loss of the system [W], can be concluded from the equation (6) as follows:

$$E_{loss} = \dot{Q}_H - \dot{Q}_S - P_{eff} \quad (6)$$

### 3. Results

#### 3.1. Heat pump efficiency

The theoretical COP is obtained using CoolPack software for the employed refrigerant R22, providing an idealized representation of the heat pump's efficiency. The p-h diagram is built by plotting the pressure and temperature data captured by sensors at a critical point in the cycle (without considering pressure and temperature drops) as shown in Figure 5A.

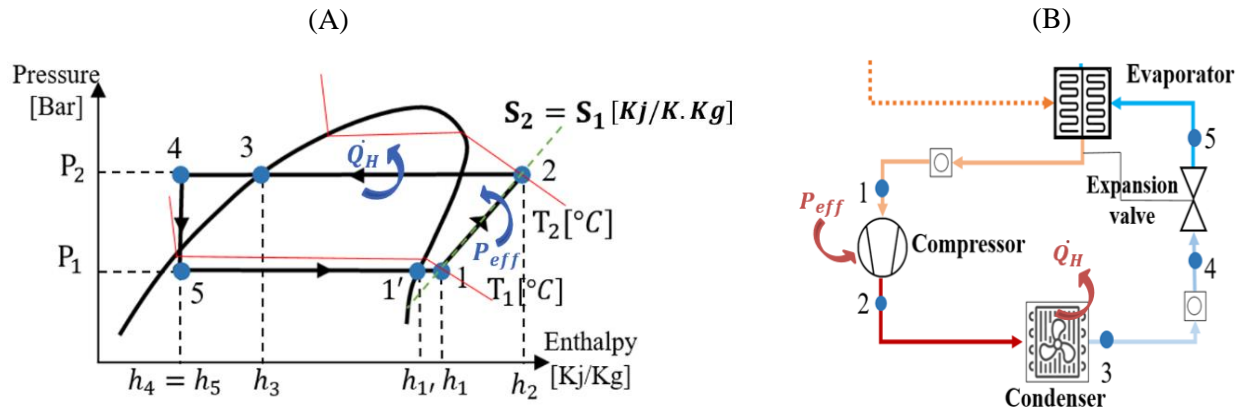


Figure 5. Schematic drawing of the experimental setup: (A) Sample p-h diagram, (B) Heat pump

We calculated the theoretical COP for each day using Equation (7):

$$COP_{HP_{theor.}} = \frac{\dot{Q}_H}{\dot{W}} = \frac{(h_2 - h_4)}{(h_2 - h_1)} \quad (7)$$

Where  $h_1$ ,  $h_2$ , and  $h_4$  are the enthalpies at specific points in the cycle, estimated with the help of the software.

The following equation was used to compute the real COP for each day based on the measured data:

$$COP_{HP_{real}} = \frac{\dot{Q}_H}{P_{eff}} \quad (8)$$

The results are illustrated in Figure 6, accompanied by grey bubbles indicating the average system loss in each scenario.

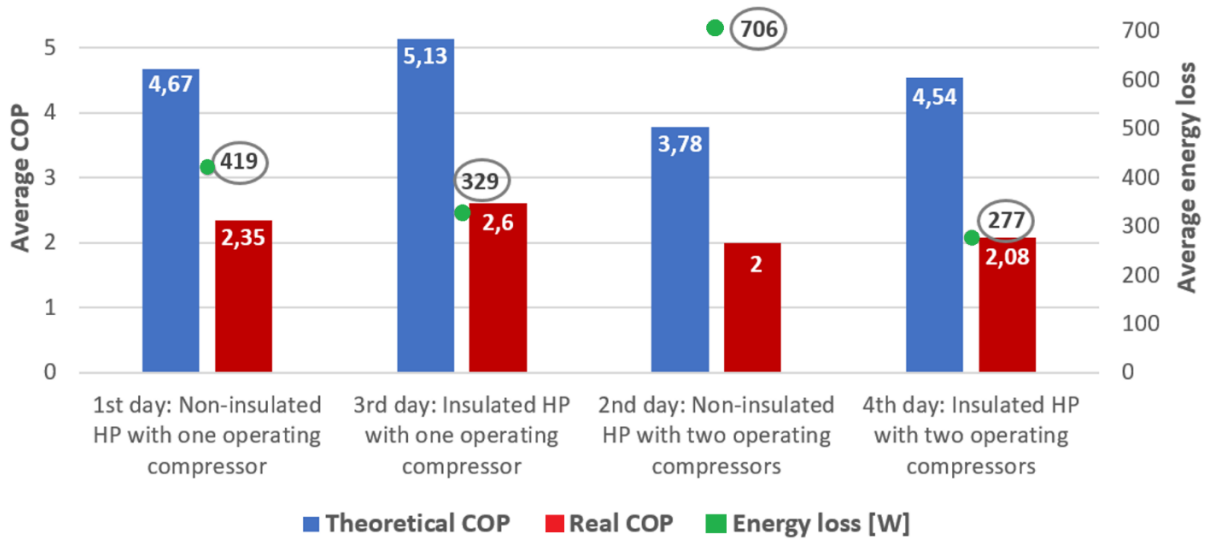


Figure 6. Average COP results and energy losses

It's evident that the theoretical COP values are higher than the real ones, attributed to measurement errors, heat dissipation, and operational parameter discrepancies. However, a consistent correlation exists between the values, with insulation consistently leading to higher COP, as observed:

On the 1<sup>st</sup> and 3<sup>rd</sup> days, the non-insulated heat pump with one operating compressor exhibited higher loss (419 W) compared to the insulated counterpart (329 W). Theoretical COPs were 4.67 and 5.13, while real COPs were 2.35 and 2.6, respectively.

On the 2<sup>nd</sup> and 4<sup>th</sup> days, the non-insulated heat pump with two operating compressors had the highest loss (706 W) among the scenarios, and the loss reached the lowest value when the insulated applied (277 W). Theoretical COPs were 3.78 and 4.54, while real COPs were 2 and 2.08, respectively.

### 3.2. System energy analysis

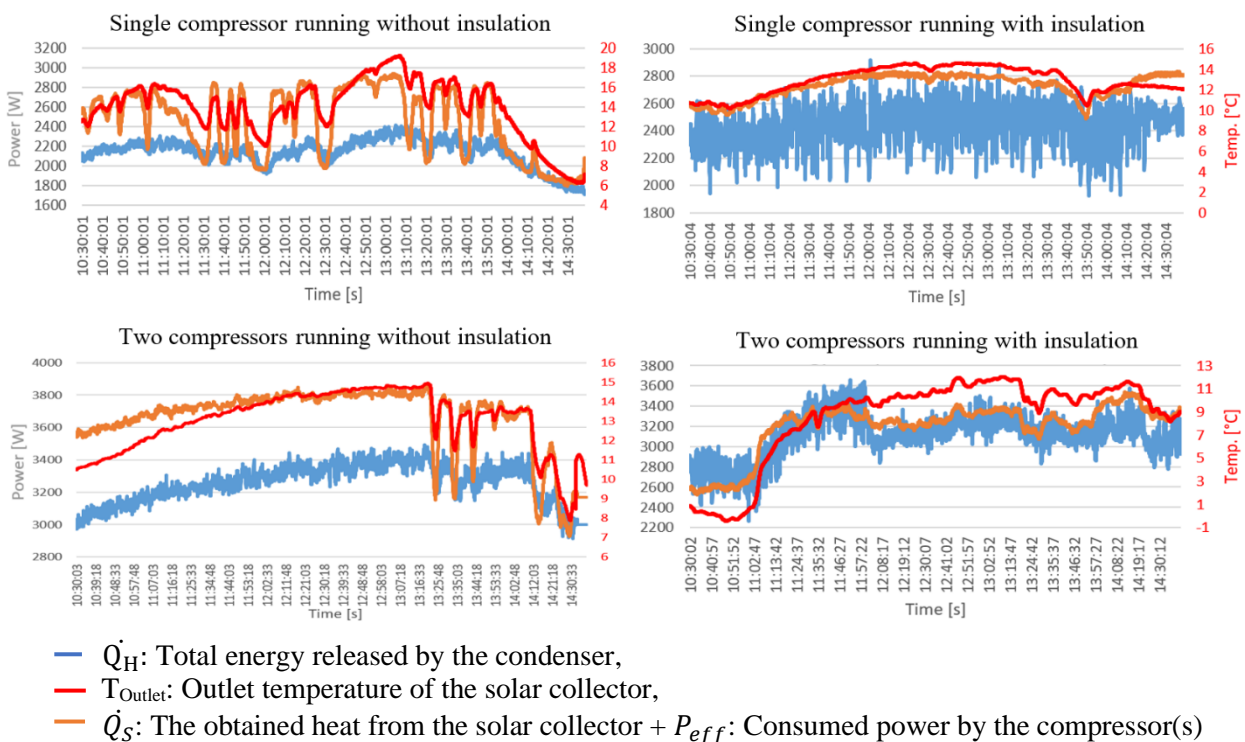


Figure 7. Energy comparison of the system

In this section, we'll understand more about the losses that occur during the system by presenting the condenser's thermal performance concerning the energy consumed by the compressor(s) and extracted heat from the solar plate, as mathematically shown in equation (1). The graphs in Figure 7 exhibit the measured energies besides the outlet temperature of the solar collector, the measurements were conducted throughout the day, however, due to data losses and transient periods, we are adopting the evaluation from 10:30 AM to 2:30 PM (a total of four hours of operation).

The graphical contrast between the orange and blue plots illustrates the energy losses in our system. The alignment is particularly pronounced on days when insulation is applied, underscoring the insulation's efficacy in mitigating losses. A correlation was found between the outlet temperature of the solar collector and the reduction in energy losses. Specifically, a lower outlet temperature corresponded to a decrease in the absorbed heat, consequently resulting in diminished overall system losses.

#### 4. Conclusions

Given that heating is a crucial energy requirement for individuals and businesses worldwide, the importance of well-designed equipment such as the SAHP system becomes essential. This not only translates into tangible cost savings but also contributes significantly to reducing carbon footprints, aligning with the global push for sustainable living. By carrying out methodical experiments and conducting a thorough analysis, we have discovered valuable insights into the operational efficiency of this technology. Our findings demonstrate that the application of insulation aids in achieving a state of perfect reversibility by minimizing energy loss caused by external thermal transformations. Additionally, increasing the operational units of the compressor can further reduce these losses. Furthermore, we discovered that the system was unable to effectively utilize the heat gained by the solar collector, when the outlet temperature of the solar collector increases, the amount of heat acquired increases as well, resulting in system losses. In conclusion, while insulation and compressor functioning are crucial factors in the SAHP, there are additional components inside the system that significantly influence overall efficiency and should be taken into consideration for future studies and designs, such as the evaporator and the solar collector.

#### Acknowledgements

This work was supported by the Stipendium Hungaricum Programme and by the Mechanical Engineering Doctoral School, The Hungarian University of Agriculture and Life Sciences, Gödöllő, Hungary.

#### References

- [1] **Omer, A. M.** (2008). Ground-source heat pumps systems and applications. *Renewable and sustainable energy reviews*, 12(2), 344-371.
- [2] **Carroll, P., Chesser, M., and Lyons, P.** (2020). Air Source Heat Pumps field studies: A systematic literature review. *Renewable and sustainable energy reviews*, 134, 110275.
- [3] **Ghabour, R., & Korzenszky, P.** (2020). Mathematical modelling and experimentation of soy wax PCM solar tank using response surface method. *Analecta Technica Szegedinensia*, 14(2), 35-42.
- [4] **Ghabour, R., Korzenszky, P.** (2021). Identifying the optimum tilting angles for solar thermal collectors using four different modelling factors in Hungary, *Mechanical Engineering Letters* 21, pp. 51-64., 14 p.
- [5] **Géczi, G., Korzenszky, P., Bense, L.** (2013). Ideális körülmények a levegő-víz hőszivattyú uszodatechnikai alkalmazása során, *Magyar Épületgépészet* 62, 7-8 pp. 7-10., 4 p.
- [6] **Géczi, G., Bense, L., Korzenszky, P.** (2014). Water Tempering of Pools Using Air to Water Heat Pump Environmental Friendly Solution, *Rocznik Ochrona Srodowiska* 16 pp. 115-128., 14 p.
- [7] **Thomas, N.** (2015). *Westring Pascal. European heat pump market and statistics report 2015*. Technical report. Brussels: The European Heat Pump Association AISBL (EHPA).
- [8] **Vorushylo, I., Keatley, P., Shah, N., Green, R., and Hewitt, N.** (2018). How heat pumps and thermal energy storage can be used to manage wind power: A study of Ireland. *Energy*, 157, 539-549.
- [9] **Korzenszky, P., Géczi, G.** (2012). Heat Pump Application in Food Technology, *Journal of Microbiology*



*Biotechnology and Food Sciences* 2: 2 pp. 493-500., 8 p.

- [10] **Ghabour, R., Korzenszky, P.** (2022). Linear model of DHW system using response surface method approach. *Tehnički Vjesnik-Technical Gazette*, 29(1), 66-72.
- [11] **Ghabour, R., Korzenszky, P.** (2023). Dynamic Modelling and Experimental Analysis of Tankless Solar Heat Process System for Preheating Water in the Food Industry. *Acta Polytechnica Hungarica* 20: 4pp. 65-83., 19 p.
- [12] **Nuntaphan, A., Chansena, C., and Kiatsiriroat, T.** (2009). Performance analysis of solar water heater combined with heat pump using refrigerant mixture. *Applied Energy*, 86(5), 748-756.
- [13] **Ghabour, R., & Korzenszky, P.** (2021). Technical and Non-Technical Difficulties in Solar Heat for Industrial Process. *Acta Technica Corviniensis-Bulletin of Engineering*, 14(3), 1-18.
- [14] **Ghabour, R., Josimović, L., Korzenszky, P.** (2021). Two Analytical Methods for Optimising Solar Process Heat System Used in a Pasteurising Plant, *Applied Engineering Letters* 6 :4 pp. 166-174., 9p.
- [15] **Fan, Y., Zhao, X., Han, Z., Li, J., Badiel, A., Akhlaghi, Y. G., and Liu, Z.** (2021). Scientific and technological progress and future perspectives of the solar assisted heat pump (SAHP) system. *Energy*, 229, 120719.
- [16] **Hermanucz, P., Géczy, G., and Barótfi, I.** (2021). Modeling and measurement methods for multi-source heat pumps. *Science, Technology and Innovation*, 14(3).